

Journal of Visualized Experiments

Confocal Microscope-Based Laser Ablation and Regeneration Assay in Zebrafish Interneuromast Cells

--Manuscript Draft--

Article Type:	Invited Methods Article - JoVE Produced Video
Manuscript Number:	JoVE60966R1
Full Title:	Confocal Microscope-Based Laser Ablation and Regeneration Assay in Zebrafish Interneuromast Cells
Section/Category:	JoVE Developmental Biology
Keywords:	Lateral line, interneuromast, neuromast, hair cell, mantle cell, supporting cell, ET20, regeneration, laser ablation, confocal, 405 nm
Corresponding Author:	Aaron Steiner Pace University Pleasantville, NY UNITED STATES
Corresponding Author's Institution:	Pace University
Corresponding Author E-Mail:	asteiner@pace.edu
Order of Authors:	Bryan A. Volpe Teresa H Fotino Aaron Steiner
Additional Information:	
Question	Response
Please indicate whether this article will be Standard Access or Open Access.	Open Access (US\$4,200)
Please indicate the city, state/province, and country where this article will be filmed . Please do not use abbreviations.	Pleasantville, New York, USA

TITLE:

Confocal Microscope-Based Laser Ablation and Regeneration Assay in Zebrafish Interneuromast Cells

AUTHORS AND AFFILIATIONS:

Bryan A. Volpe, Teresa H. Fotino, Aaron B. Steiner

Department of Biology, Pace University, Pleasantville, NY, USA

Corresponding Author:

Aaron B. Steiner (asteiner@pace.edu)

Email Addresses of Co-authors:

Bryan A. Volpe (bv98841p@pace.edu)

Teresa H. Fotino (tfotino@frontier.com)

KEYWORDS:

lateral line, interneuromast, neuromast, hair cell, mantle cell, supporting cell, ET20, regeneration, laser ablation, confocal, 405 nm

SUMMARY:

Laser ablation is a widely applicable technology for studying regeneration in biological systems. The presented protocol describes use of a standard laser-scanning confocal microscope for laser ablation and subsequent time-lapse imaging of regenerating interneuromast cells in the zebrafish lateral line.

ABSTRACT:

Hair cells are mechanosensory cells of the inner ear that mediate the sense of hearing. These cells do not regenerate after damage in humans, but they are naturally replenished in non-mammalian vertebrates such as zebrafish. The zebrafish lateral line system is a useful model for characterizing sensory hair cell regeneration. The lateral line is comprised of hair cell-containing organs called neuromasts, which are linked together by a string of interneuromast cells (INMCs). INMCs act as progenitor cells that give rise to new neuromasts during development. INMCs can repair gaps in the lateral line system due to cell death, necessitating an experimental protocol for characterizing such regeneration. A method is described here for selective INMC ablation using a conventional laser-scanning confocal microscope and transgenic fish that express green fluorescent protein in INMCs. Time-lapse microscopy is then used to monitor INMC regeneration and determine the rate of gap closure. This represents an accessible protocol for cell ablation that does not require specialized equipment, such as a high-powered pulsed ultraviolet laser. The ablation protocol may serve broader interests, as it could be useful for the ablation of additional cell types, employing a tool set that is already available to many users. This technique will further enable the characterization of INMC regeneration under different conditions and from different genetic backgrounds, which will advance the understanding of sensory progenitor cell regeneration.

INTRODUCTION:

At the core of most progressive hearing loss lies the destruction of sensory hair cells, which transduce extrinsic auditory stimuli into nerve impulses detectable by the brain. Cochlear hair cell death causes permanent hearing loss, as adult mammals lack the ability to regenerate these cells following damage. Conversely, non-mammalian vertebrates such as zebrafish can regenerate hair cells lost to acoustic trauma or ototoxic insult. The zebrafish mechanosensory lateral line is a simple and easily manipulated organ system that can be used to study hair cell regeneration¹⁻³.

The lateral line consists of small sensory patches called neuromasts, which are connected during development by a string of elongated cells known as interneuromast cells (INMCs). Given their proliferative capacity as apparent stem cells that give rise to new hair cell-containing organs, the behavior of INMCs is of great interest to the community^{4,5}. Much of the research pertaining to INMCs has characterized their suppression by nearby Schwann cells that wrap around the lateral line nerve as well as proliferative behavior following the knockdown of associated signaling pathways such as Wnt/ β -catenin⁶⁻⁸. While the regulation of INMC proliferation and differentiation into new neuromasts has been well-described, the mechanisms governing INMC regrowth after ablation have not been elucidated. This protocol serves as a means of ablating individual INMCs and analyzing their subsequent regenerative behavior.

A variety of methods for destroying hair cells, supporting cells, and entire neuromasts have been published, along with methodologies for monitoring recovery. Chemical ablation works well for hair cells, but doses of toxic chemicals such as CuSO₄ must be significantly increased to remove other lateral line cell types⁹. While electroablation under fluorescence microscopy is an effective and simple means of destroying INMCs to study regeneration, it is difficult to target narrowly and, therefore, is likely to produce significant collateral damage. As a result, this can mask aspects of INMC-specific behaviors^{10,11}. Laser ablation protocols have been employed, but they require the use of specialized equipment not necessarily present in the average laboratory or imaging facility (i.e., high-powered pulsed UV lasers¹²). The method described here can be performed with any laser-scanning confocal microscope outfitted with the common 405 nm laser, usually used for imaging DAPI and other blue fluorophores. An advantage of this method is that confocal imaging can be performed immediately before and after cell damage without engaging any additional laser control systems or transferring to another microscope equipped with a pulsed laser.

A similar method has been described for ablating neurons in the zebrafish spinal cord¹³. However, the previous method requires a FRAP module for cell ablation, which is not a requirement for this protocol. Furthermore, given the distinct properties of different cell types (i.e., brightness of transgene fluorescence, depth within the body, and cell shape), it is likely that significant modifications will be needed depending on the cell type used. The protocol detailed here is more likely to be effective for more superficial cells, as supported by a demonstration of sensory hair cell ablation using the same method. Also outlined is a

regeneration assay to assess INMC recovery rates after ablation, which was not a feature of the aforementioned study.

The laser-based cell ablation protocol detailed herein captures the regenerative capacity of INMCs through the optimization of laser conditions, pre- and post-ablation imaging, and time-lapse microscopy. These elements come together to comprehensively portray INMC regrowth and gap closure in its entirety. While this protocol is used here to destroy INMCs, it may be applied to other work that requires reliable and effective assessment of cellular ablation. It is also an accessible technology, since it can be conducted on any confocal microscope equipped with a 405 nm laser.

PROTOCOL:

All animal work was approved by the Pace University Institutional Animal Care and Use Committee under protocol 2018-1.

1. Preparation of zebrafish larvae

1.1. Set up mating 3–5 days prior to conducting the experiment, such that larvae will be 2 days post-fertilization (dpf) to 4 dpf in age when mounted for laser ablation.

NOTE: The *Et(krt4:EGFP)sqEt20* (abbreviated as ET20) enhancer trap line, in which interneuromast cells are clearly labeled with enhanced green fluorescent protein (eGFP), allows for relatively easy cell identification and ablation^{11,14}. For confirmation of laser ablation specificity and flexibility, ET20 fish are bred with *Tg(neuroD:tdTomato)* fish, in which the lateral line nerve is labeled with red fluorescent protein or with *Tg(myo6b:βactin-GFP)* to label sensory hair cells with GFP^{15,16}.

1.2. After embryo collection the following day, incubate embryos at 28.5 °C in E3 medium containing 0.0001% methylene blue until ready to anesthetize and mount.

2. Preparation of low gelling agarose and tricaine solutions

2.1. To a 250 mL glass Erlenmeyer flask, add 48 mL of 1x E3 medium, 2 mL of 15 mM tricaine stock solution, and 0.5 g of low-melting agarose.

2.2. Microwave the solution on high for 30 s and swirl (wearing heat-protective gloves) to dissolve the agarose. Repeat the 30 s heating cycles until agarose is fully dissolved.

2.3. Store the agarose in an incubator heated to 42 °C until ready to use.

3. Anesthetization of zebrafish larvae

3.1. To a 50 mL conical tube, add 24 mL of 1x E3 medium and 1 mL of tricaine stock solution (15

mM) to a final concentration of 600 μ M. Swirl to mix.

3.2. Load one of the six wells of a flat-bottomed cell culture plate with 8 mL of E3 containing 600 μ M tricaine.

3.3. Use a transfer pipette to move zebrafish larvae into a 74 μ m mesh-bottomed transfer insert.

3.4. Transfer the mesh-bottomed insert into the well of the six-well plate containing the E3 + tricaine solution. Allow the larvae to remain in the well for a minimum of 3 min or until fully anesthetized. Test anesthesia by tapping the insert. Larvae should not startle and swim in response to the tap.

4. Fluorescent screening of anesthetized zebrafish larvae

4.1. Pipette one anesthetized larva per well onto 12 well hydrophobic-coated slides for screening. Ensure that there is minimal curvature of the meniscus formed in each well of the slide to reduce optical distortion when screening. This can be done by removing a small volume of E3 from each well after placing the larvae.

4.2. Under a 10x objective on an upright microscope (equipped with a mercury arc lamp, metal-halide lamp, or LED light source and an appropriate filter cube), screen for larvae that express eGFP in the neuromasts and interneuromast cells of the lateral line system.

4.2.1. Select larvae with stronger expression resulting in brighter eGFP, which presumably are homozygous for the transgene.

NOTE: In the ET20 line, eGFP is expressed in a ring of mantle cells surrounding each neuromast, as well as, the narrow strip of interneuromast cells connecting these organs. Stronger eGFP expression (brighter fluorescence) contributes to more effective ablation.

4.2.2. To examine the specificity of ablation, use double-transgenic larvae with both the ET20 and *Tg(neuroD:tdTomato)* transgenes. If screening for *Tg(neuroD:tdTomato)* carriers, use the RFP filter cube set to identify a bright red patch just posterior to the ear representing the posterior lateral line ganglion.

4.2.3. To ablate hair cells in the lateral line neuromasts, use the *Tg(myo6b: β actin-GFP)* transgenic line and screen for GFP localization in the center of each neuromast.

4.3. Select larvae with stereotypical spacing of the neuromasts. Differences in the spacing between neuromasts may indicate abnormal neuromast deposition during development, suggesting defective migratory behavior or cell proliferation in the lateral line primordium¹⁷. Such defects may also affect migratory or regenerative behavior of the INMCs following ablation.

NOTE: Common defects in spacing include an unusually large distance between the anterior-most neuromast deposited by the first migrating primordium (prim1L1) and the second neuromast deposited by the same primordium (prim1L2), often associated with crowding of the more posterior neuromasts.

5. Mounting larvae for laser ablation and imaging

5.1. Pipette 3 - 4 anesthetized larvae into a small droplet of E3/tricaine solution in the center of a cover slip-bottomed dish (35 mm dish with a 14 mm number 1.5 coverslip). Remove excess solution so that the larvae remain in a small droplet, just large enough to contain them.

5.2. Transfer the dish to the stage of a binocular stereo microscope and manipulate the zoom and focus so that all larvae are in the field of view.

5.3. Remove the Erlenmeyer flask containing the low melting point agarose from the heated incubator. Use a transfer pipette to transfer agarose solution onto the cover slide to produce a thin layer. Draw off excess agarose until the liquid just fills the well at the bottom of the dish, taking care not to aspirate any larvae.

5.4. Quickly arrange the larvae in the agarose solution using a hair knife or hair loop so that they are aligned with each other and oriented with rostral to the left.

5.5. Gently press the larvae down against the glass with the hair knife, such that they lie in profile with their right sides down. Larvae older than 3 dpf tend to float due to their inflated swim bladders, so they may need to be repeatedly pressed down against the glass until the agarose begins to gel.

5.6. After about 60 s, the agarose will start to solidify, and the larvae will not be able to be reoriented. Allow approximately 5 min at room temperature for the agarose on the cover slide to completely solidify. Once the agarose has solidified, use a transfer pipette to fill the dish halfway with E3 containing 1x tricaine.

6. Locating prospective targets and pre-ablation imaging

6.1. Turn on the power to the laser-scanning confocal microscopy system and initialize through the integrated imaging software. Select the 63x Plan-Apochromat oil immersion objective (numerical aperture 1.40) or similar. Apply immersion oil and secure the dish in a circular stage insert such that the larvae face with their rostral aspect to the left.

6.2. Under bright-field or differential interference contrast illumination, select one of the mounted larvae for imaging. Adjust the focus with the focus knob such that the skin on the side of the fish closest to the coverslip is in focus, recognizable by the fingerprint-like pattern of periderm cells.

6.3. Once in focus, switch to epifluorescent illumination in the GFP channel. Locate the posterior lateral line by GFP expression along the horizontal myoseptum. Rings of fluorescent cells indicate neuromast mantle cells, and elongated strands of cells are interneuromast cells.

6.4. Beginning with the primIL1 neuromast, usually located just dorsal to the yolk, use the stage control joystick or other stage movement control to visually scan caudally along the horizontal myoseptum.

6.4.1. Follow the string of interneuromast cells until reaching the region between the primIL3 and primIL4 (L3 and L4) neuromasts (**Figure 1A**).

NOTE: Other regions can also be targeted, but this section of the trunk and tail tends to be closest to the cover glass and, therefore, most amenable to ablation.

6.4.2. If imaging several larvae, set the first stage position, then inactivate the multiple stage positions option by deselecting the appropriate check box.

6.4.3. Repeat steps 6.4.1–6.4.2. for each desired stage position (each larva).

6.5. After cell bodies in the L3–L4 region have been identified, switch to the acquisition mode.

6.5.1. Activate a GFP imaging track using the 488 nm or 491 nm laser.

6.5.2. Add a transmitted light (transmitted light photomultiplier tube or T-PMT) channel to the activated 488 nm laser track by activating the T-PMT checkbox under the “**Imaging Setup**” dropdown menu.

6.5.3. Set the laser power to 6%, pinhole size to 1 Airy unit equivalent, and digital gain to 750 for imaging ET20 larvae. Exact gain and laser power may vary for any given larva, depending upon how close to the cover slip they are mounted and the brightness of fluorescence. Adjust the gain such that cell bodies are saturated to capture otherwise dim projections and filipodia.

6.5.4. Adjust the parameters to a frame size of 1024 pixels x 1024 pixels, digital zoom of 0.7 (145.2 μm x 145.2 μm image size). Set averaging to 2 to improve image quality.

6.6. Check the z-stack box to bring up the z-position dropdown menu. While fast scanning, focus out until the interneuromast cells are just out of focus. Set the first slice, then focus through the sample until the interneuromast cells are once again out of focus. Set the last slice. Ensure that it encompass a z-stack of approximately 25 μm . Set the imaging interval to 1 μm .

6.7. Start experiment to capture a pre-ablation z-stack (**Figure 1B**). If stage positions have been added, inactivate the positions option so that only the current position is imaged. Save the file once it is captured.

7. Laser ablation of cell bodies

7.1. Click on **“Show all Tools”**. This option is located at the top of the acquisition interface.

7.2. Click on the dropdown menu for **“Imaging Set Up”**. In **“Imaging Set up”**, click on **“Add a new track”** (represented as **“+”**).

7.3. In **“Imaging Set Up”**, click on the dropdown menu for **“Dye”**. Select DAPI as the dye.

7.4. Click on the dropdown menu for **“Channels”** and deselect all other tracks by unclicking their respective checkboxes. Ensure that only the DAPI track is selected.

7.5. In the DAPI track, click on 405 for the **“Laser setting”**. Increase the laser power to 75%. Unclick the DAPI channel to turn off the laser while scanning for candidate cell bodies for ablation.

7.6. With the body of an interneuromast cell centered in the field of view, zoom in the scanning frame to 20x–22x. The frame position may need to be adjusted to keep the cell body in the center as the zoom is applied. Stop live scanning as soon as the cell body fills the field of view.

NOTE: The cell body should occupy the entire field of view. At this zoom level, the GFP will bleach rapidly. Minimize laser exposure time by working quickly. Use zoom rather than selecting a region of interest to increase laser power distribution over a small area.

7.7. Check the 405 nm laser shutter box to activate the track. Adjust the laser power to 75%. Set a timer for 45 s. Activate continuous scanning and start the timer. Stop scanning immediately at 45 s.

8. Post-ablation imaging and time-lapse microscopy to study regeneration

8.1. Click on the dropdown menu for **“Channels”**. In channels, unclick the **“DAPI”** track to inactivate the ablation laser. Click on the dropdown menu for **“Acquisition mode”**.

8.2. In acquisition mode, click on **“Zoom”**.

8.3. Decrease the zoom to 0.7 either by using the slider or by typing in **“0.7.”**

8.3.1. To ensure successful cell ablation, increase the gain to 900 and fast scan the field of view.

NOTE: No GFP should be visible within the targeted cell or cells. If fluorescence is still observed, return to steps 7.1–7.3.

8.3.2. Using the same or similar settings as those described for pre-ablation imaging, capture

and save a post-ablation image (**Figure 1C**). If the image reveals remnants of fluorescent cells or additional cell bodies that needs to be removed, repeat the laser ablation steps to create a visible gap in the string of interneuromast cells.

8.3.3. Inspect the T-PMT channel image to further confirm cellular damage. Damaged cells will have a granular appearance, and frequently the nuclei will swell or become irregular in shape (**Figure 2**).

8.4. After capturing a pre-ablation image, ablating the cells as necessary, and capturing a post-ablation image for each individual stage position, set up the time-lapse microscopy by activating both stage position and time options for image capture. Set the time parameters to 24 h or another desired endpoint and 15 min intervals. Start experiment to acquire images and save the resulting file when complete (on the following day).

8.5. If larvae are to be further studied or raised, carefully remove them from the agarose using fine forceps, then transfer into E3 medium without tricaine for recovery. If they are not to be used further, euthanize according to the approved animal protocol (rapid and sustained immersion in an ice bath is a common method) and dispose of them as required by the institution.

9. Image analysis

9.1. Open a post-ablation z-stack file in the preferred image processing software (**Table of Materials**). Split the channels such that each channel is in a separate viewing pane.

9.2. In the GFP channel window, use the line tool to draw a straight line between the tips of the remaining INMCs. This may be aided by scrolling up and down through the z-stack or by performing a maximum-intensity projection prior to drawing the line.

9.3. Use the “**Measure**” tool to obtain the distance between INMC ends in the x- and y-planes.

9.4. Scroll through the z-slices in the original z-stack to determine the distance between INMCs in the z-plane.

9.5. Calculate the total distance between INMC ends using the Pythagorean theorem ($a^2 + b^2 = c^2$). The hypotenuse is the total distance (or gap size).

9.6. Enter the resulting distance measurement into a spreadsheet application for data analysis.

9.7. Review the time-lapse microscopy files collected in step 8.2–8.3 using either the integrated imaging software on the confocal system or freely available image analysis software. Identify the timepoint at which the gap between interneuromast cells was filled in by cell projections. This can be aided by examination of multiple z-slices to confirm closure of the gap in all dimensions.

9.8. To achieve the most accurate measurement of time to gap closure, use the post-ablation image time stamp (visible in Finder or File Explorer) as the zero time point; measuring time from the beginning of the time-lapse image stack may result in underestimating time to closure, depending upon how much time elapsed while ablating additional stage positions, etc.

9.9. Derive the rate of closure by simply dividing the original gap size (μm) by the hours or minutes required for complete gap closure.

REPRESENTATIVE RESULTS:

In order to ablate INMCs and record regeneration, screened GFP-expressing zebrafish larvae of the ET20 transgenic line were mounted at 2- or 3-days post-fertilization for ablation as described in step 5.4. Several fish can be mounted simultaneously so that multiple time lapses can be captured in a single experiment. The region of the lateral line located between primIL3 and primIL4 neuromasts was identified, and pre-ablation images were captured as described in steps 6.5–6.7 (**Figure 1A,B**).

Three cell bodies were targeted for laser ablation to create a gap in the INMC string of approximately 40 μm . Post-ablation scanning with high gain and subsequent imaging confirmed that no cell bodies remained in the ablated region, leaving a gap between elongated projections of the adjacent INMCs (**Figure 1C**). Cell death was further demonstrated by examining the T-PMT channel after ablation. Damaged and dying cells were marked by swollen and irregularly shaped nuclei as well as a granular appearance (**Figure 2**, outlined). In some cases, time-lapse imaging also revealed the recruitment of large amoeboid cells that were likely macrophages (**Figure 2**, asterisk). Dark areas surrounding the ablated INMCs indicated photobleaching in overlying periderm cells. These cells did not appear to be damaged or destroyed by laser irradiation in these experiments; rather, their fluorescence was temporarily reduced. Time-lapse microscopy reveals that these cells normally recover after ablation and do not change shape or otherwise appear damaged (unpublished results, Volpe et al.).

To support the specificity of INMC destruction, ablations were performed in double-transgenic ET20 and *Tg(neuroD:tdTomato)* larvae in which the lateral line nerve (which runs just microns below the interneuromast cells) is labeled with red fluorescent protein. Ablations of several cells that created sizeable gaps in the INMC string had little or no effect on the lateral line nerve based on red fluorescence (**Figure 3**). Flexibility of the technique for ablating superficially localized cells was demonstrated by selective destruction of individual sensory hair cells within neuromasts of the lateral line. Using essentially the same protocol detailed above (sections 7 and 8), single hair cells in transgenic *Tg(myo6b:βactin-GFP)* larvae were destroyed without apparent damage to adjacent cells (**Figure 4**). The ablated hair cells did not recover fluorescence after time-lapse microscopy, and their nuclei were noticeably granular and misshapen after laser exposure (**Figure 4B**). Similar to INMC ablations, apparent macrophages were frequently recruited to the laser exposure site (unpublished results, Volpe et al.).

Following laser ablation and post-ablation image capture, gap size was measured using freely available image analysis software. The measure tool demonstrated gap sizes ranging from just a few microns up to 100 microns, depending upon the width of individual INMCs and how many cells were chosen for ablation (**Figure 5**). Timelapse microscopy was employed to record INMC behaviors during regeneration. In 50 trials, 15 gaps (30%) were closed by regeneration within a 24 h period. In most cases, INMCs that were able to recover did so within the first several hours of imaging. Recovery was defined as the timepoint at which projections from neighboring cells came into contact, which occurred 8 h after ablation for a gap of approximately 40 μm (**Movie 1**). Z-stacks were carefully examined to ensure that cell-cell contact occurred within a single z-plane, avoiding possible artifacts due to z-projections. Logistic regression analysis revealed that the probability of gap closure correlated with gap size ($p = 0.453$), with smaller gaps being more likely to heal. A gap of 55.5 μm yielded a closure probability of 50% (**Figure 5**).

In 70% of cases, INMCs were unable to completely close the gap created by ablation. However, even in these cases we were able to monitor the formation of long projections from neighboring INMCs, which resemble in some respects extending neuronal growth cones (**Movie 2**). Thus, these experiments can also provide insight into the behaviors of INMCs after damage.

FIGURE AND TABLE LEGENDS:

Figure 1: Selective ablation of interneuromast cells by laser irradiation. (A) Interneuromast cells between neuromasts primIL3 and primIL4 were selected for ablation. These cells display a characteristic spindle shape with elongated projections overlapping adjacent cell bodies. (B) Pre-ablation imaging identified cell bodies that could be ablated to produce a gap. (C) Post-ablation imaging confirms successful ablation as indicated by the absence of cell bodies in the gap region. Scale bars = 10 μm .

Figure 2: Post-ablation imaging demonstrates cell death in response to laser exposure in GFP-labeled interneuromast cells. Transmitted light photomultiplier imaging (T-PMT) indicates the presence of a necrotic cell with a granular appearance (encircled), as well as, the recruitment of irregularly shaped cells that are likely macrophages (*). Merging of GFP and T-PMT channels confirms that cell death and macrophage activity occurred at the site of ablation. Scale bars = 10 μm .

Figure 3: Specificity of interneuromast ablation. (A) Pre-ablation GFP-labeled interneuromast cells (green) and tdTomato-labeled lateral line nerve (red) in a double-transgenic *Tg(ET20;NeuroD:tdTomato)* larva. Cell bodies in close proximity to the lateral line nerve were targeted for ablation. (B) Post-ablation imaging demonstrates ablation of targeted cell bodies with an intact lateral line nerve. Scale bars = 10 μm .

Figure 4: Ablation of sensory hair cells using confocal microscopy. (A) Pre-ablation imaging identified a GFP labeled sensory hair cell (*) targeted for ablation in double-transgenic *Tg(ET20;myo6b:βactin-GFP)* zebrafish. Transmitted light photomultiplier tube (T-PMT) imaging discloses normal hair cell morphology, with a round cross-section. (B) Post-ablation imaging confirms

successful ablation of the targeted hair cell. A T-PMT image indicates irregularity in hair cell shape and increased granularity after laser exposure, suggesting cell death rather than photobleaching. Scale bars = 10 μ m.

Figure 5: Logistic regression modeling the probability of gap closure as a function of gap width (in μ m) in RStudio. A score of 0 represents complete gap closure, whereas a score of 1 represents incomplete gap closure. Results indicate that the effect of gap width on the ability of interneuromast cells to close respective gaps is statistically significant ($p = 0.0453$, $n = 24$ total; $n = 12$ closed gaps, $n = 12$ incompletely closed gaps).

Movie 1: Time-lapse microscopy demonstrating gap closure (~40 μ m) after 16 h. Images were captured every 30 min, and a maximum-intensity z-projection was made for all timepoints.

Movie 2: Time-lapse microscopy of an INMC gap that did not close. The elongated and branching projections of the remaining INMCs are shown.

DISCUSSION:

The protocol describes a versatile method for laser cell ablation that can be performed on any confocal microscope equipped with a near-ultraviolet laser (405 nm wavelength). This protocol addresses limitations of previously employed methods such as electroablation (which causes more widespread damage¹¹) and pulsed UV-laser ablation (which requires additional specialized equipment¹²). Pre- and post-ablation confocal imaging provide rapid feedback regarding success of the experiment. Subsequent time-lapse microscopy offers a simple assay for regeneration in a cell type critical for sensory system development.

It is of vital importance to prescreen for transgenic zebrafish that express GFP strongly in neuromasts and INMCs. Larvae with bright fluorescence and approximately even spacing of the prim1-derived neuromasts are ideal candidates for laser ablation. Even in these fish, there are occasionally dimmer INMCs that may at first escape detection. These cells can remain behind after laser ablation, preventing the formation of a true gap between INMCs. The digital gain should be adjusted to reveal these dimmer cells during pre-ablation imaging such that they can also be targeted with the 405 nm laser (step 8.2).

Similarly, laser targeting sometimes will not entirely destroy a cell; rather, it will bleach the fluorescence, resulting in a failure to create a real gap. These cells will generally increase in fluorescence during timelapse microscopy. Gain adjustment in the post-ablation imaging step along with T-PMT imaging (**Figure 2**) help ensure that all cells targeted have been effectively removed. It frequently requires two or three individual cell ablations to produce a gap in the INMC string. Cell death can be detected by blebbing or a granular appearance in the targeted cells; although, this may require a brief waiting period after laser targeting (and in some cases, apparent apoptotic or necrotic figures are observed shortly thereafter).

A limitation of this procedure is that it may require multiple experimental trials before laser conditions are optimized and INMC regeneration is successful. The laser power and total dwell

time of the laser may each require slight adjustment for different samples. It has been found that excessive laser application can impair the ability of the lateral line to repair itself. This includes both 1) overexposure of individual cells to laser irradiation, presumably causing additional damage to surrounding tissues, as well as 2) the ablation of too many cells in the string, leading to a larger gap. Users must achieve a balance between sufficiently irradiating cells to ensure their destruction and not overexpose the cells, which can slow or prevent regeneration. With the appropriate settings, it has been found that the INMCs can be removed without visible damage to the posterior lateral line nerve, indicating that collateral damage is minimized with this protocol unlike electroablation¹¹. In no cases were new neuromasts forming in the gap observed, presumably because the lateral line nerve remains intact and underlying glial cells remain and inhibit the proliferation of INMCs^{6-8,11}.

It is demonstrated that this method of confocal laser ablation may be applied to other cell types as well, particularly in those superficially located within the animal including sensory hair cells (**Figure 4**). A similar protocol may be used to ablate skin cells to examine wound repair or neurons for axonal regeneration studies, as previously described¹³. It is anticipated that this technique will become a useful addition to the experimental repertoire of laboratories that possess a confocal microscope but no other specialized equipment for laser ablation.

ACKNOWLEDGMENTS:

This work was funded by NIH R15 grant 1R15DC015352-01A1 and Pace University internal funding sources. Fish lines were courtesy of Vladimir Korzh¹⁴, Katie Kindt^{15,16}, and the laboratory of A. James Hudspeth. We would like to thank A. James Hudspeth and members of his group for feedback on these experiments, and colleagues at Pace University for their support. Logistic regression analysis in RStudio was aided in particular by our colleague Matthew Aiello-Lammens.

DISCLOSURES:

The authors have nothing to disclose.

REFERENCES:

- 1 Denans, N., Baek, S., Piotrowski, T. Comparing Sensory Organs to Define the Path for Hair Cell Regeneration. *Annual Review Cell & Developmental Biology*. **35**, 567-589 (2019).
- 2 Ghysen, A., Dambly-Chaudiere, C. The lateral line microcosmos. *Genes & Development*. **21** (17), 2118-2130 (2007).
- 3 Lush, M. E., Piotrowski, T. Sensory hair cell regeneration in the zebrafish lateral line. *Dev Dyn*. **243** (10), 1187-1202 (2014).
- 4 Ledent, V. Postembryonic development of the posterior lateral line in zebrafish. *Development*. **129** (3), 597-604 (2002).
- 5 Nunez, V. A. et al. Postembryonic development of the posterior lateral line in the zebrafish. *Evolution and Development*. **11** (4), 391-404 (2009).
- 6 Grant, K. A., Raible, D. W., Piotrowski, T. Regulation of latent sensory hair cell precursors by glia in the zebrafish lateral line. *Neuron*. **45** (1), 69-80 (2005).
- 7 Lopez-Schier, H., Hudspeth, A. J. Supernumerary neuromasts in the posterior lateral line

529 of zebrafish lacking peripheral glia. *Proceedings of the National Academy of Sciences U. S. A.*
530 **102** (5), 1496-1501 (2005).

531 8 Lush, M. E., Piotrowski, T. ErbB expressing Schwann cells control lateral line progenitor
532 cells via non-cell-autonomous regulation of Wnt/beta-catenin. *eLife*. **3**, e01832 (2014).

533 9 Hernandez, P. P. et al. Sublethal concentrations of waterborne copper induce cellular
534 stress and cell death in zebrafish embryos and larvae. *Biological Research*. **44** (1), 7-15 (2011).

535 10 Moya-Diaz, J. et al. Electroablation: a method for neurectomy and localized tissue injury.
536 *BMC Developmental Biology*. **14**, 7 (2014).

537 11 Sanchez, M., Ceci, M. L., Gutierrez, D., Anguita-Salinas, C., Allende, M. L.
538 Mechanosensory organ regeneration in zebrafish depends on a population of multipotent
539 progenitor cells kept latent by Schwann cells. *BMC Biology*. **14** 27, (2016).

540 12 Viader-Llargues, O., Lupperger, V., Pola-Morell, L., Marr, C., Lopez-Schier, H. Live cell-
541 lineage tracing and machine learning reveal patterns of organ regeneration. *eLife*. **7**, (2018).

542 13 Morsch, M. et al. Triggering Cell Stress and Death Using Conventional UV Laser Confocal
543 Microscopy. *Journal of Visualized Experiments*. (120), e54983 (2017).

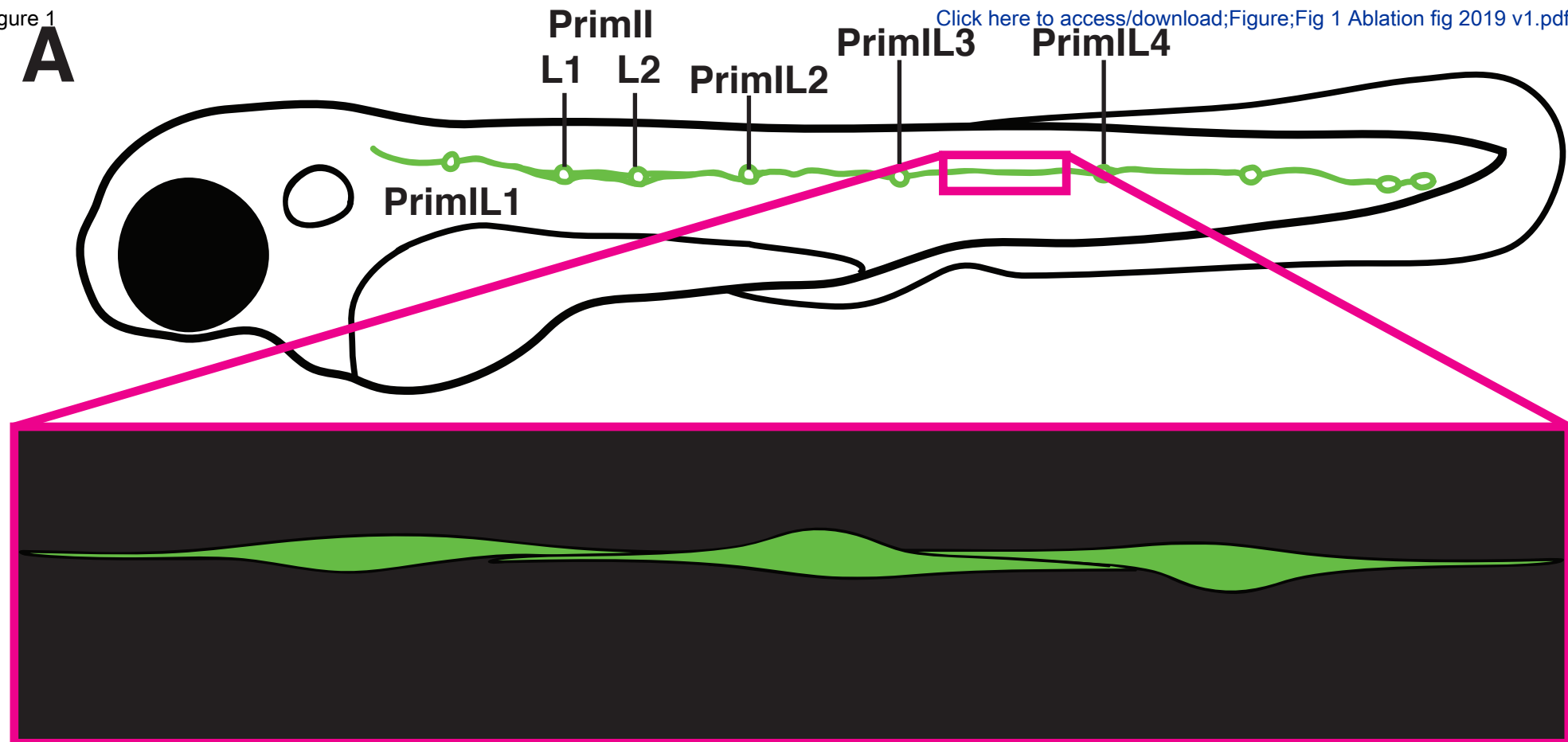
544 14 Parinov, S., Kondrichin, I., Korzh, V., Emelyanov, A. Tol2 transposon-mediated enhancer
545 trap to identify developmentally regulated zebrafish genes in vivo. *Developmental Dynamics*
546 **231** (2), 449-459 (2004).

547 15 Kindt, K. S., Finch, G., Nicolson, T. Kinocilia mediate mechanosensitivity in developing
548 zebrafish hair cells. *Developmental Cell*. **23** (2), 329-341 (2012).

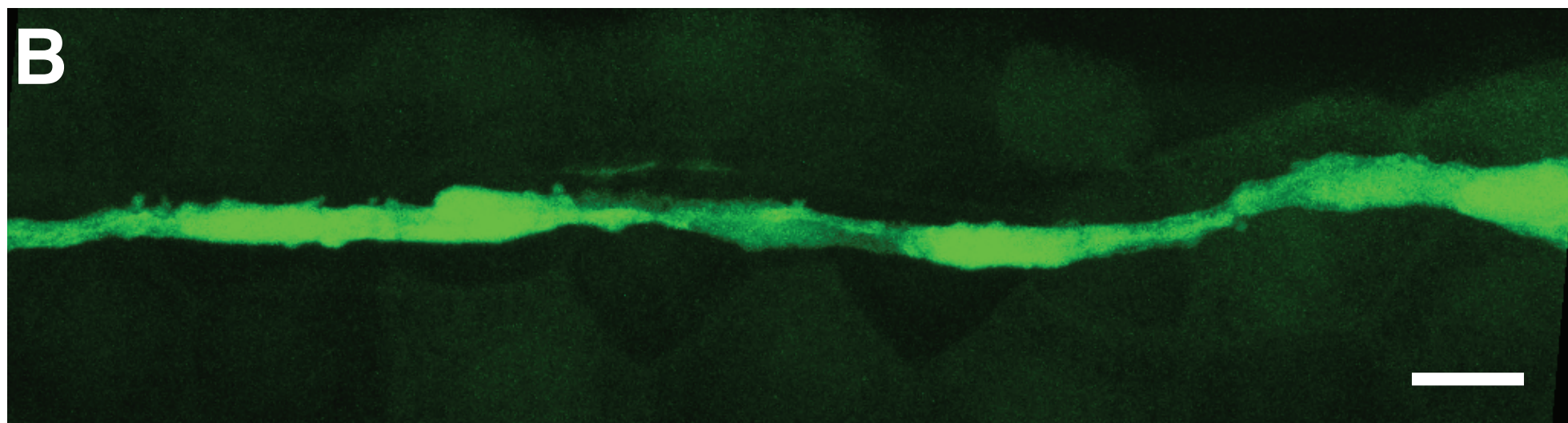
549 16 Toro, C. et al. Dopamine Modulates the Activity of Sensory Hair Cells. *Journal of*
550 *Neurosciences*. **35** (50), 16494-16503 (2015).

551 17 Dalle Nogare, D., Chitnis, A. B. A framework for understanding morphogenesis and
552 migration of the zebrafish posterior Lateral Line primordium. *Mechanisms of Development*. **148**,
553 69-78 (2017).

A



B



C

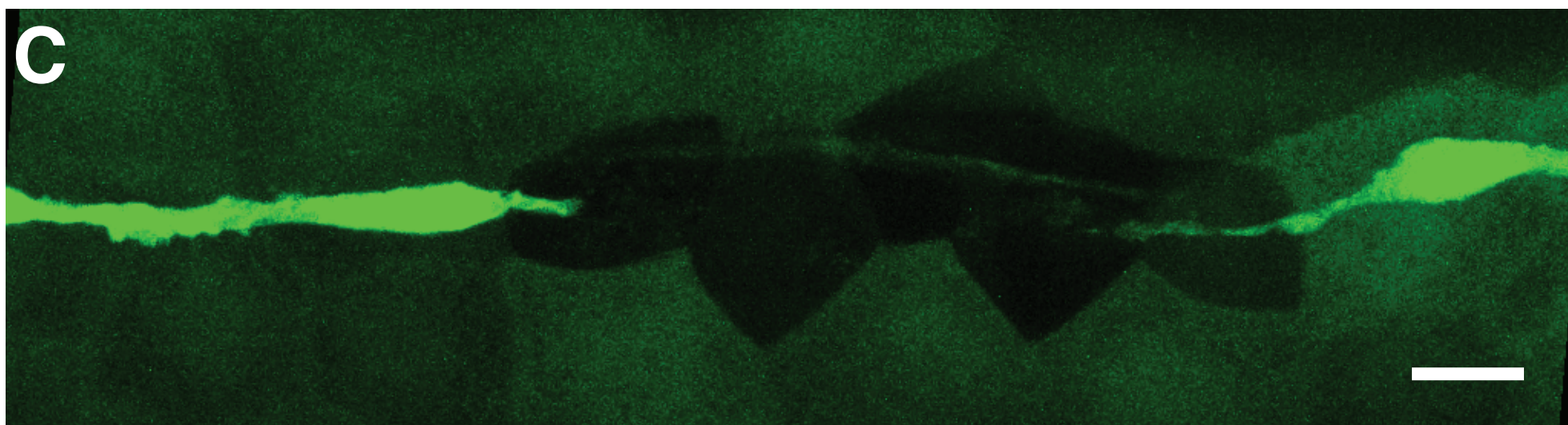


Figure 2

[Click here to access/download;Figure;Fig 2 Dying cell v2.pdf](#) 

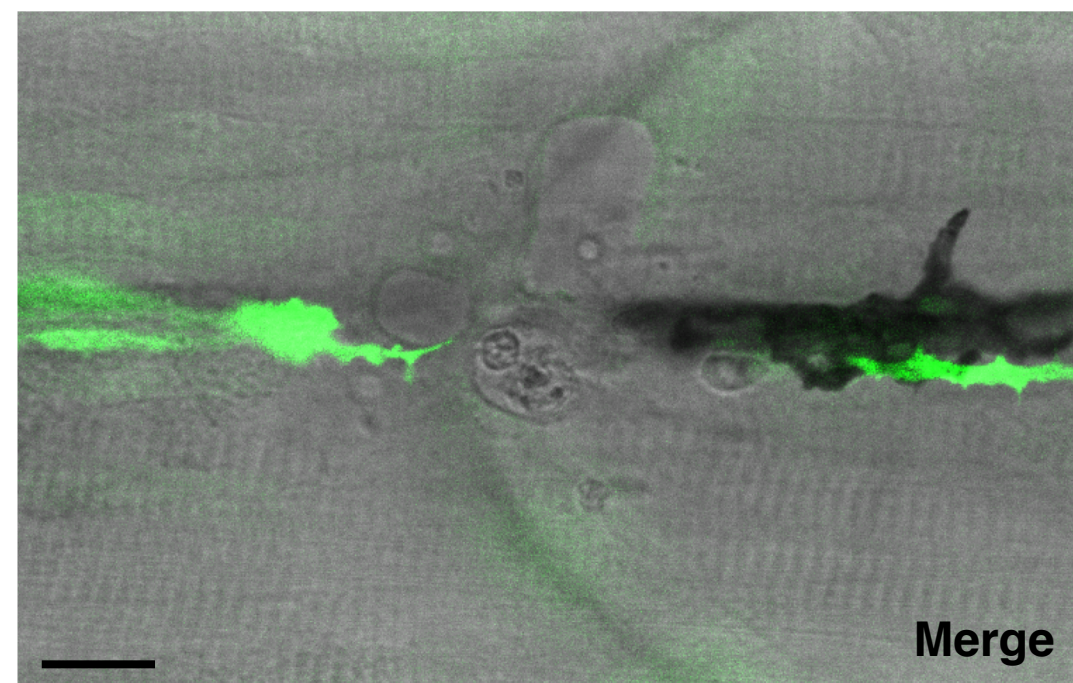
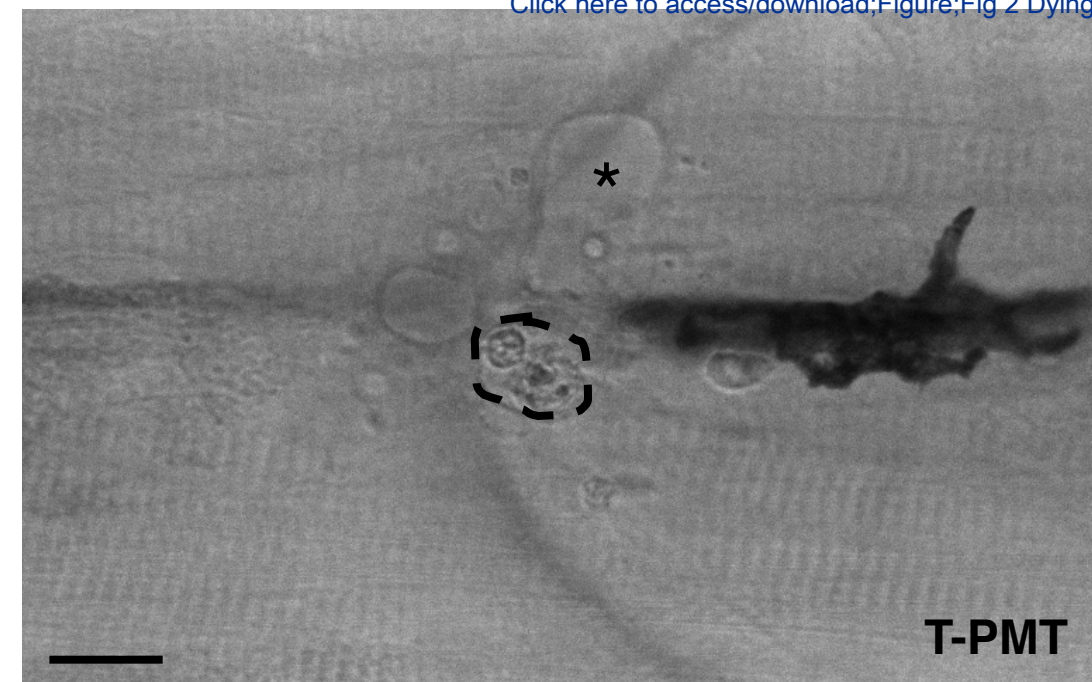
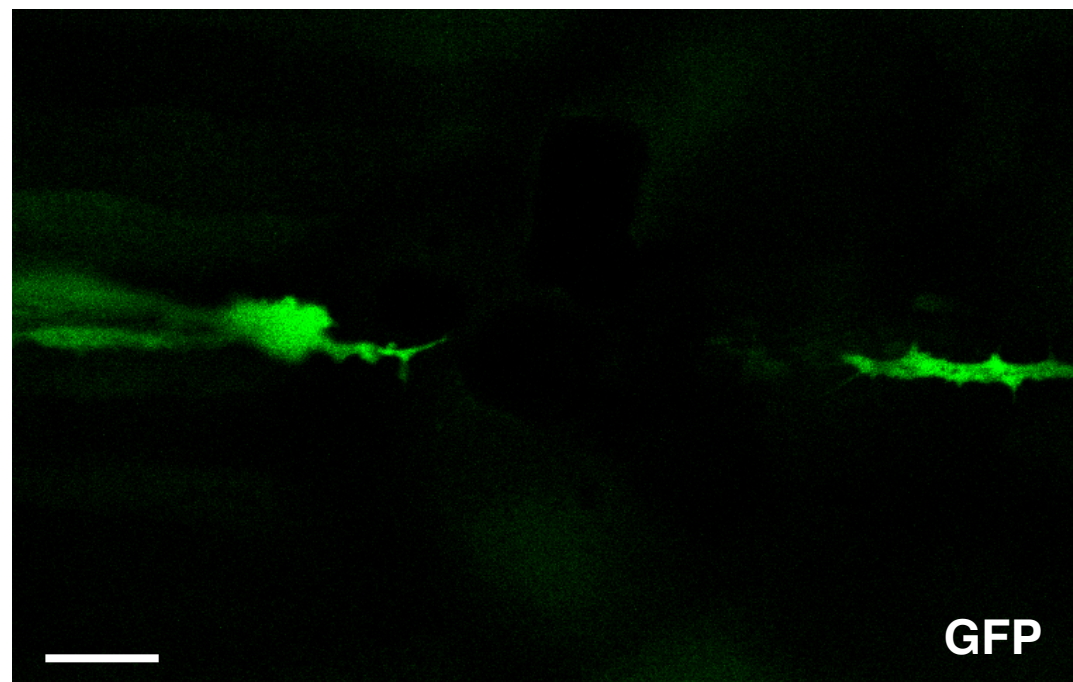


Figure 3

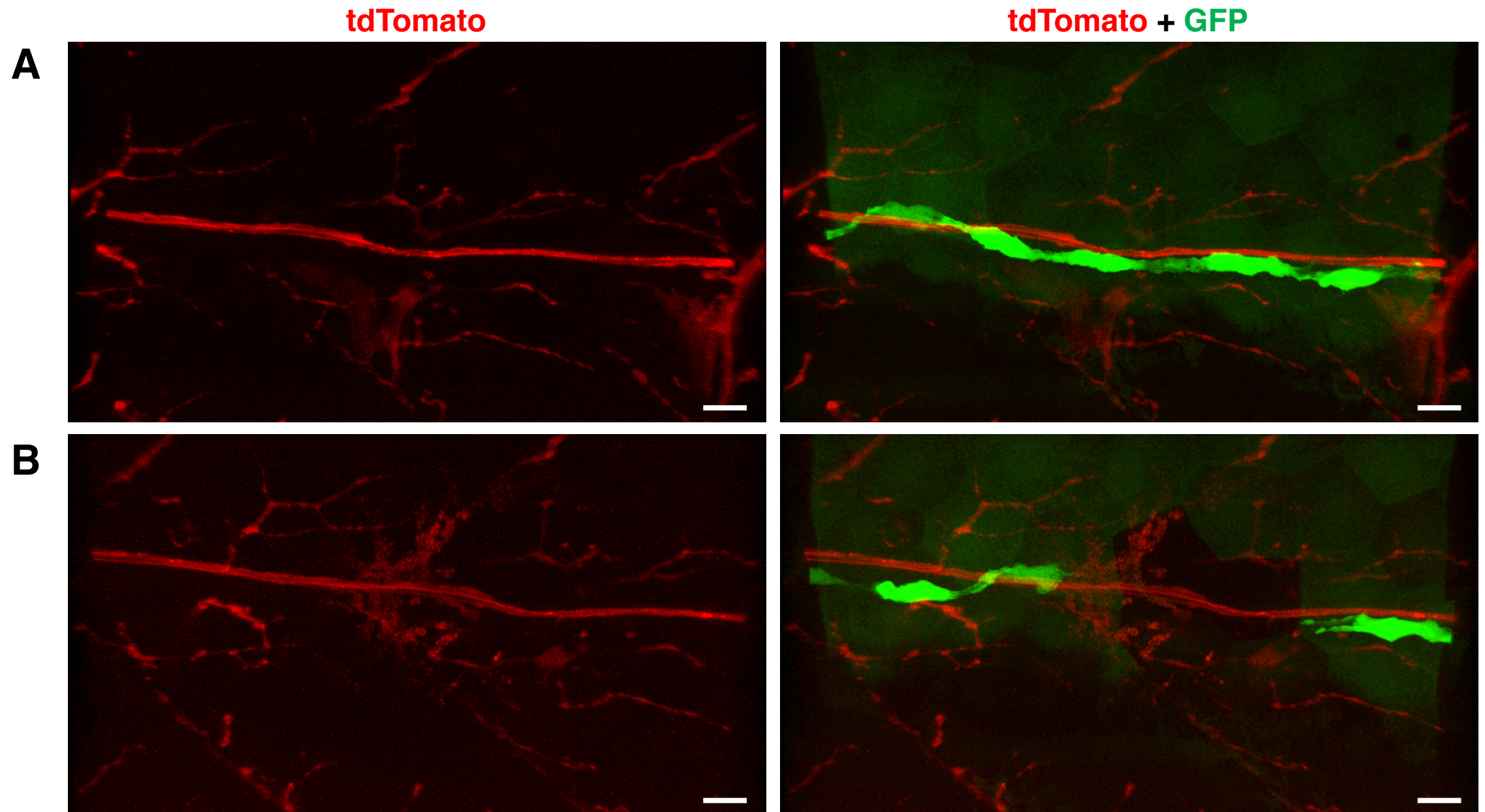


Figure 4

[Click here to access/download;Figure;Figure 4 HC ablation figure v2.pdf](#)

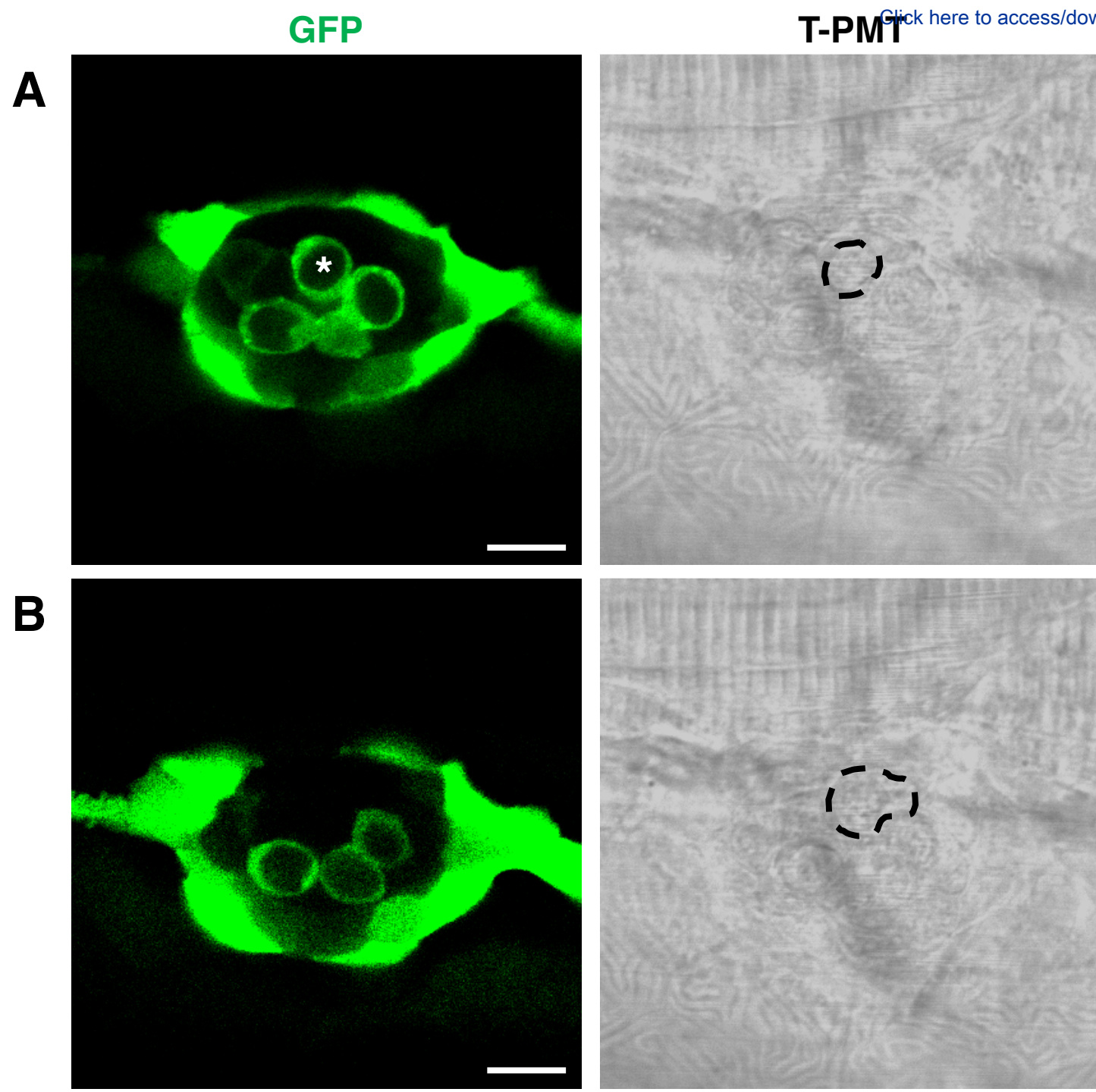
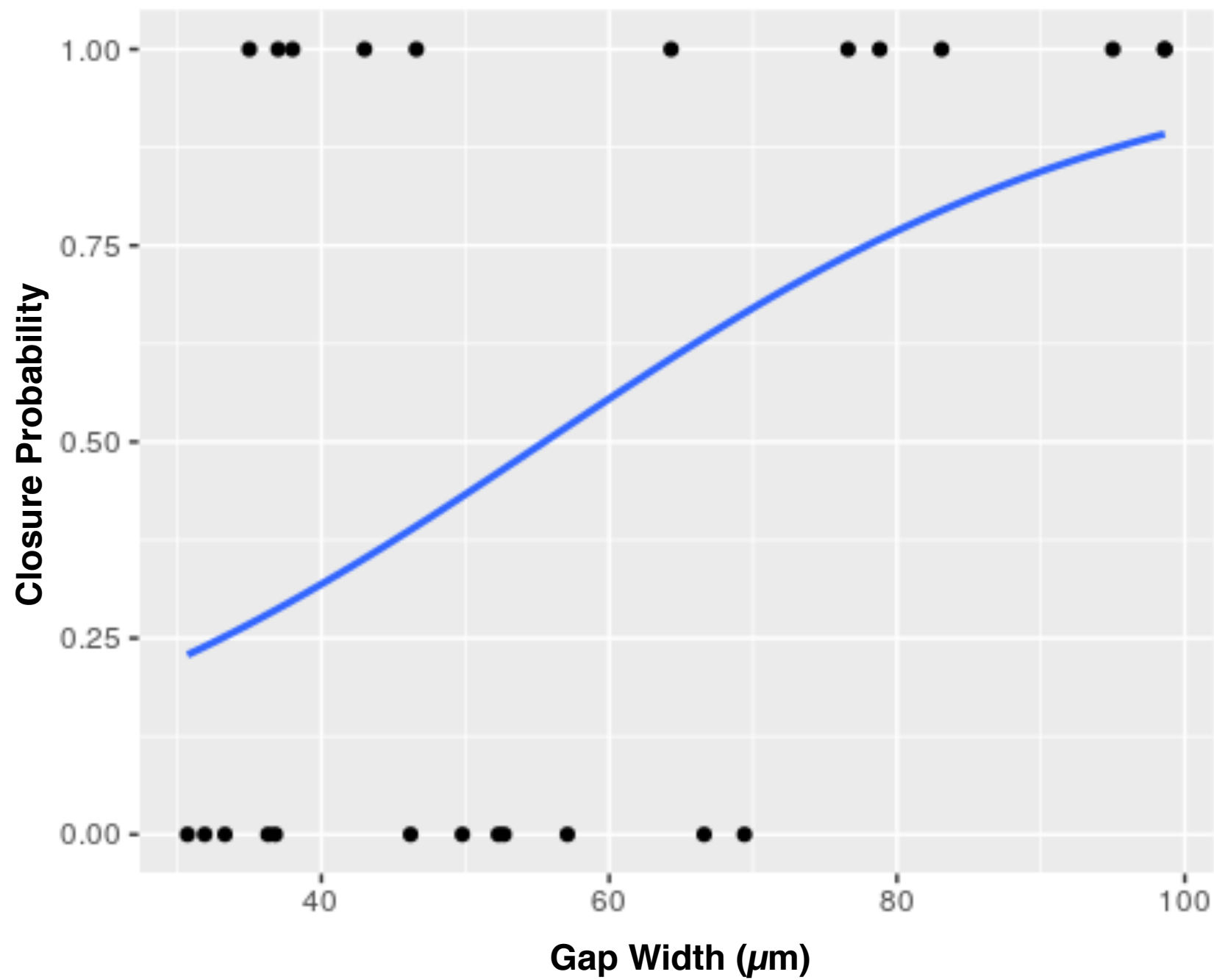
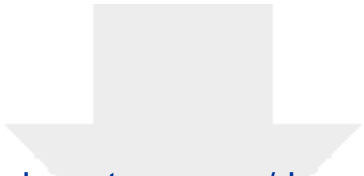


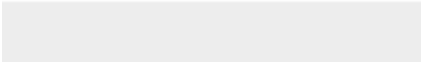

Figure 5

[Click here to access/download;Figure;Fig 5 Gap closure logistic regression.pdf](#)



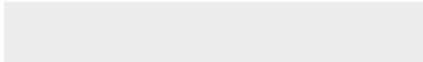



Click here to access/download
Video or Animated Figure
Suppl Movie 1.avi





Click here to access/download
Video or Animated Figure
Suppl Movie 2.avi



Name of Material/Equipment	Company	Catalog Number
12-well PTFE Printed Slides	Electron Microscopy Sciences	63425-05
15 mM Tricaine stock solution	Sigma	E10521
1X E3 + 600 μ M Tricaine		
1X E3 media		
60 X E3 media	All components purchased from Sigma-	
Bx60 Compound microscope with mercury arc lamp fluorescence	Olympus	
LSM 700 confocal microscope equipped with 405 nm, 488 nm, and 555 or 561 nm lasers	Carl Zeiss Microscopy, LLC	
FIJI/ImageJ Image processing software	Multiple contributors	
Dissecting needle modified into hair knife	Fisher Scientific	19010
Microsoft Excel software	Microsoft Corp.	
Glass bottom 35 mm dishes with no. 1.5 coverslip, 20 mm window	Mattek Corporation	P35G-1.5-20-C
Immersol 518F Immersion Oil	Fisher Scientific	12-624-66A
Low Gelling Agarose	Sigma Life Science	A9414-256
Corning Netwell Insert with 74 μ m Polyester Mesh, 24 mm Insert	Millipore Sigma	CLS3479-48EA
Rstudio software	Rstudio PBC	
SMX-168-BL Stereo microscope	Motic	
Transfer Pipette	Fisher Scientific	13-711-7M
ZEN software	Carl Zeiss Microscopy, LLC	

Comments/Description

15 mM Tricaine in reverse osmosis water

Dilute 15 mM Tricaine stock 25X in 1X E3 media

Dilute 60X E3 media to 1X in reverse osmosis water (16.7 ml/L)

34.4 g NaCl, 1.52 g KCl, 5.8 g $\text{CaCl}_2 \cdot 2\text{H}_2\text{O}$, 9.8 g $\text{MgSO}_4 \cdot 7\text{H}_2\text{O}$ in 1 liter reverse-osmosis

A 5 mW 405 nm laser was used for ablation; Ablations and imaging were performed through a 63x Plan-Apochromat objective with an NA of 1.40

Downloadable at <https://fiji.sc/>

An eyelash was glued onto the end of a wood-handled dissecting needle

Google sheets is a no-cost alternative to Microsoft Excel

35 mm petri dish, 20 mm glass window

Downloadable at <https://rstudio.com/>



DYSON COLLEGE OF ARTS & SCIENCES
Department of Biology
861 Bedford Road
Pleasantville, NY 10570
(914) 773-3587

February 3, 2020

Dr. Kyle Jewhurst
Journal of Visualized Experiments
1 Alewife Center, Suite 200
Cambridge, MA 02140

Dear Dr. Jewhurst,

Please find attached our resubmission of the manuscript, "A confocal microscope-based laser ablation and regeneration assay for zebrafish interneuromast cells," JoVE 60966. We appreciate the editorial comments and valuable feedback from the reviewers, and feel that this review process has allowed us to considerably strengthen our manuscript. We have addressed to the best of our ability the majority of concerns raised by reviewers, including the following major concerns:

- We have included data representing 50 trials of our protocol to support reliability and reproducibility.
- Figure 1, which was described as not "particularly useful or interesting" has been replaced.
- Additional figures and Results have been added to demonstrate the efficacy of cell ablation and the minimal damage to surrounding tissues.
- An additional figure was added to represent use of this technique for ablating a different cell type (sensory hair cells), demonstrating flexibility and broader applicability.

We have also made every effort to adhere to the editorial review comments by removing commercial language and personal pronouns, as well as other suggestions made by the editors. This revision was developed in consultation with all coauthors, each of whom has approved of this final version. Please let us know if you have any remaining questions or concerns regarding our resubmitted manuscript.

Best Regards,



Aaron B. Steiner, Ph.D.
asteiner@pace.edu



DYSON COLLEGE OF ARTS & SCIENCES
Department of Biology
861 Bedford Road
Pleasantville, NY 10570
(914) 773-3587

February 4, 2020

Dr. Kyle Jewhurst
Journal of Visualized Experiments
1 Alewife Center, Suite 200
Cambridge, MA 02140

Dear Dr. Jewhurst, Dr. Bajaj, and Editorial Staff,

Please find attached our resubmission of the manuscript, "A confocal microscope-based laser ablation and regeneration assay for zebrafish interneuron cells," JoVE 60966. We appreciate the editorial comments and valuable feedback from the reviewers, and feel that this review process has allowed us to considerably strengthen our manuscript. We have addressed to the best of our ability the concerns raised by reviewers, as detailed below.

Editorial comments:

1. We have thoroughly proofread the manuscript to ensure that there are no typographical or grammatical errors.
2. We have removed commercial language from the protocol, relegating all such information to the revised Table of Materials.
3. We have changed the text of the protocol to use the imperative tense in each step.
4. We have removed personal pronouns from the protocol; some personal pronouns remain in the Results and Discussion sections, but presumably this is not an issue.
5. We have broken down some of the longer steps into simpler, 2-3 step procedures.
6. We believe that we have been explicit in describing how each step is performed.
7. In step 5.1, we have added that the fish are anesthetized for this step.
8. We have broken down steps 5.4, 6.4, and 6.5 into sub-steps for simplicity.
9. We have not broken down step 7 into individual mouse clicks because these are commonly used tools in confocal microscopy, and entering each mouse click would surely make the protocol well over the ten page limit. We feel that we have provided enough detail for the casual confocal microscope user to follow. If the editors feel that these still need to be broken down further, we will do so at the expense of brevity.
10. We have highlighted approximately 2.75 pages of the protocol, but are happy to reduce the highlighted portion further if we have inadvertently included too many steps for filming.
11. None of our figures have been previously published in any form.
12. The figure legends each include a title and a short description of the data included therein.

Reviewer 1:

Major concerns: None

Minor concerns:

1. We have included a new figure demonstrating cell death after laser irradiation (Figure 2) and have added step 8.2 to ensure that the cell is no longer fluorescing after ablation.
2. We have added a figure (Figure 3) to demonstrate that nearby tissues, namely the lateral line nerve, are unaffected by focused laser ablation. We have further added a section in the representative results section (lines 344-348) detailing the photobleaching and survival of periderm cells.

3. We have added the specifications of the 405 nm laser to both the protocol (Step 7.1) and the Table of Materials.
4. The reason for using high zoom rather than a region of interest for ablation is now included in Step 7.2 (lines 255-256).
5. We have modified our protocol to use the freely-available FIJI software package for analyzing gap size, eliminating the costly Imaris software (section 9).
6. We have removed the term “failed experiments” from our manuscript (lines 375-378).
7. We have completed both incomplete sentences pointed out by the Reviewer (Steps 6.1 and 7.3, formerly step 7.2).

Reviewer 2:

Major concerns:

1. Figure 1, referred to as not “particularly useful or interesting,” has been replaced.
2. Figure 3 has also been replaced.
3. We have provided data showing that the targeted cells die (Figure 2) and that the ablation is selective (Figure 3).
4. We have included data on the reproducibility of the results and the likelihood of gap closure (lines 366 and 375, Figure 5) as well as evidence of cell death (Figure 2).
5. We have addressed the question regarding the advantage of our technique over electroablation (greater selectivity) and the observation of new neuromast formation in a previous study (lines 454-459).
6. We have removed the steps in which larvae are rinsed with E3 medium as suggested.
7. We have provided additional details on the imaging setup, including the pinhole size (step 6.5.3) and numerical aperture of the objective (step 6.1 and Table of Materials). We have also explained why we use high zoom for ablations (step 7.2).
8. As described above, we have switched out the costly Imaris software for FIJI in our image analysis section (section 9).
9. We have provided results for 50 trials (30% closure rate) and the correlation between gap size and likelihood of gap closure (Figure 5) as evidence of reproducibility.
10. We now make reference to additional previous studies in our Discussion section (line 426, 427, 457, 459).

Minor concerns:

1. We have completed the two incomplete sentences noted by the Reviewer (Steps 6.1 and 7.3, formerly step 7.2).

Reviewer 3:

Major concerns:

1. We have demonstrated hair cell ablation as an additional application of our technique (Figure 4).
2. We are uncertain what is meant by “the legal implications of the work.” Does this refer to animal care and use? As mentioned on lines 99-100, all animal work was approved by the Institutional Animal Care and Use Committee. This would presumably vary from institution to institution, but we have no knowledge of how such experiments would be considered by different committees, nor in different countries.

Minor concerns:

1. Figure 1 has been replaced.

Reviewer 4:

Major concerns:

1. We have now included a figure showing that the ablated cell is dying, and that apparent macrophages are recruited to remove the cellular debris (Figure 2).

Minor concerns:

1. We have added a period to the sentence cited on line 112.
2. We have removed the E3 rinses from our protocol.
3. The sentence cited as line 192 has been completed.
4. The positions option (lines 216-216) will vary depending upon the software in use; however, it is impossible to address what this option may be called in all possible software packages. We do refer to the specific software used to perform this protocol in the Table of Materials.
5. We have completed the sentence formerly on line 240, now line 253.
6. We were unable to identify the font change mentioned; we believe that the entire manuscript is in the correct font.
7. As described above, we have added a period to the offending sentence.
8. We have replaced the word “removed” with “destroyed” on line 442.
9. It is unclear what is meant by “what the differences are” between neuromasts in figure 2. These are simply the common annotations for sequential neuromasts along the lateral line.
10. The mesh wells for transferring zebrafish larvae are listed in the Table of Materials and will appear in the accompanying video.

This revision was developed in consultation with all coauthors, each of whom has approved of this final version. Please let us know if you have any remaining questions or concerns regarding our resubmitted manuscript.

Best Regards,

A handwritten signature in black ink, appearing to read 'A. Steiner', with a long, horizontal flourish extending to the right.

Aaron B. Steiner, Ph.D.
asteiner@pace.edu

ARTICLE AND VIDEO LICENSE AGREEMENT

Title of Article:	A confocal microscope-based laser ablation and regeneration assay for zebrafish interneuromast cells
Author(s):	Bryan A. Volpe, Teresa Fotino, and Aaron B. Steiner

Item 1: The Author elects to have the Materials be made available (as described at <http://www.jove.com/publish>) via:

☐

Standard Access

☒

Open Access

Item 2: Please select one of the following items:

☒

The Author is **NOT** a United States government employee.

☐

The Author is a United States government employee and the Materials were prepared in the course of his or her duties as a United States government employee.

ARTICLE AND VIDEO LICENSE AGREEMENT

1. **Defined Terms.** As used in this Article and Video License Agreement, the following terms shall have the following meanings: “**Agreement**” means this Article and Video License Agreement; “**Article**” means the article specified on the last page of this Agreement, including any associated materials such as texts, figures, tables, artwork, abstracts, or summaries contained therein; “**Author**” means the author who is a signatory to this Agreement; “**Collective Work**” means a work, such as a periodical issue, anthology or encyclopedia, in which the Materials in their entirety in unmodified form, along with a number of other contributions, constituting separate and independent works in themselves, are assembled into a collective whole; “**CRC License**” means the Creative Commons Attribution-Non Commercial-No Derivs 3.0 Unported Agreement, the terms and conditions of which can be found at: <http://creativecommons.org/licenses/by-nc-nd/3.0/legalcode>; “**Derivative Work**” means a work based upon the Materials or upon the Materials and other pre-existing works, such as a translation, musical arrangement, dramatization, fictionalization, motion picture version, sound recording, art reproduction, abridgment, condensation, or any other form in which the Materials may be recast, transformed, or adapted; “**Institution**” means the institution, listed on the last page of this Agreement, by which the Author was employed at the time of the creation of the Materials; “**JoVE**” means MyJoVE Corporation, a Massachusetts corporation and the publisher of The Journal of Visualized Experiments; “**Materials**” means the Article and / or the Video; “**Parties**” means the Author and JoVE; “**Video**” means any video(s) made by the Author, alone or in conjunction with any other parties, or by JoVE or its affiliates or agents, individually or in collaboration with the Author or any other parties, incorporating all or any portion

of the Article, and in which the Author may or may not appear.

2. **Background.** The Author, who is the author of the Article, in order to ensure the dissemination and protection of the Article, desires to have the JoVE publish the Article and create and transmit videos based on the Article. In furtherance of such goals, the Parties desire to memorialize in this Agreement the respective rights of each Party in and to the Article and the Video.

3. **Grant of Rights in Article.** In consideration of JoVE agreeing to publish the Article, the Author hereby grants to JoVE, subject to **Sections 4 and 7** below, the exclusive, royalty-free, perpetual (for the full term of copyright in the Article, including any extensions thereto) license (a) to publish, reproduce, distribute, display and store the Article in all forms, formats and media whether now known or hereafter developed (including without limitation in print, digital and electronic form) throughout the world, (b) to translate the Article into other languages, create adaptations, summaries or extracts of the Article or other Derivative Works (including, without limitation, the Video) or Collective Works based on all or any portion of the Article and exercise all of the rights set forth in (a) above in such translations, adaptations, summaries, extracts, Derivative Works or Collective Works and (c) to license others to do any or all of the above. The foregoing rights may be exercised in all media and formats, whether now known or hereafter devised, and include the right to make such modifications as are technically necessary to exercise the rights in other media and formats. If the “Open Access” box has been checked in **Item 1** above, JoVE and the Author hereby grant to the public all such rights in the Article as provided in, but subject to all limitations and requirements set forth in, the CRC License.

ARTICLE AND VIDEO LICENSE AGREEMENT

4. **Retention of Rights in Article.** Notwithstanding the exclusive license granted to JoVE in **Section 3** above, the Author shall, with respect to the Article, retain the non-exclusive right to use all or part of the Article for the non-commercial purpose of giving lectures, presentations or teaching classes, and to post a copy of the Article on the Institution's website or the Author's personal website, in each case provided that a link to the Article on the JoVE website is provided and notice of JoVE's copyright in the Article is included. All non-copyright intellectual property rights in and to the Article, such as patent rights, shall remain with the Author.

5. **Grant of Rights in Video – Standard Access.** This **Section 5** applies if the "Standard Access" box has been checked in **Item 1** above or if no box has been checked in **Item 1** above. In consideration of JoVE agreeing to produce, display or otherwise assist with the Video, the Author hereby acknowledges and agrees that, Subject to **Section 7** below, JoVE is and shall be the sole and exclusive owner of all rights of any nature, including, without limitation, all copyrights, in and to the Video. To the extent that, by law, the Author is deemed, now or at any time in the future, to have any rights of any nature in or to the Video, the Author hereby disclaims all such rights and transfers all such rights to JoVE.

6. **Grant of Rights in Video – Open Access.** This **Section 6** applies only if the "Open Access" box has been checked in **Item 1** above. In consideration of JoVE agreeing to produce, display or otherwise assist with the Video, the Author hereby grants to JoVE, subject to **Section 7** below, the exclusive, royalty-free, perpetual (for the full term of copyright in the Article, including any extensions thereto) license (a) to publish, reproduce, distribute, display and store the Video in all forms, formats and media whether now known or hereafter developed (including without limitation in print, digital and electronic form) throughout the world, (b) to translate the Video into other languages, create adaptations, summaries or extracts of the Video or other Derivative Works or Collective Works based on all or any portion of the Video and exercise all of the rights set forth in (a) above in such translations, adaptations, summaries, extracts, Derivative Works or Collective Works and (c) to license others to do any or all of the above. The foregoing rights may be exercised in all media and formats, whether now known or hereafter devised, and include the right to make such modifications as are technically necessary to exercise the rights in other media and formats. For any Video to which this **Section 6** is applicable, JoVE and the Author hereby grant to the public all such rights in the Video as provided in, but subject to all limitations and requirements set forth in, the CRC License.

7. **Government Employees.** If the Author is a United States government employee and the Article was prepared in the course of his or her duties as a United States government employee, as indicated in **Item 2** above, and any of the licenses or grants granted by the Author hereunder exceed the scope of the 17 U.S.C. 403, then the rights granted hereunder shall be limited to the maximum

rights permitted under such statute. In such case, all provisions contained herein that are not in conflict with such statute shall remain in full force and effect, and all provisions contained herein that do so conflict shall be deemed to be amended so as to provide to JoVE the maximum rights permissible within such statute.

8. **Protection of the Work.** The Author(s) authorize JoVE to take steps in the Author(s) name and on their behalf if JoVE believes some third party could be infringing or might infringe the copyright of either the Author's Article and/or Video.

9. **Likeness, Privacy, Personality.** The Author hereby grants JoVE the right to use the Author's name, voice, likeness, picture, photograph, image, biography and performance in any way, commercial or otherwise, in connection with the Materials and the sale, promotion and distribution thereof. The Author hereby waives any and all rights he or she may have, relating to his or her appearance in the Video or otherwise relating to the Materials, under all applicable privacy, likeness, personality or similar laws.

10. **Author Warranties.** The Author represents and warrants that the Article is original, that it has not been published, that the copyright interest is owned by the Author (or, if more than one author is listed at the beginning of this Agreement, by such authors collectively) and has not been assigned, licensed, or otherwise transferred to any other party. The Author represents and warrants that the author(s) listed at the top of this Agreement are the only authors of the Materials. If more than one author is listed at the top of this Agreement and if any such author has not entered into a separate Article and Video License Agreement with JoVE relating to the Materials, the Author represents and warrants that the Author has been authorized by each of the other such authors to execute this Agreement on his or her behalf and to bind him or her with respect to the terms of this Agreement as if each of them had been a party hereto as an Author. The Author warrants that the use, reproduction, distribution, public or private performance or display, and/or modification of all or any portion of the Materials does not and will not violate, infringe and/or misappropriate the patent, trademark, intellectual property or other rights of any third party. The Author represents and warrants that it has and will continue to comply with all government, institutional and other regulations, including, without limitation all institutional, laboratory, hospital, ethical, human and animal treatment, privacy, and all other rules, regulations, laws, procedures or guidelines, applicable to the Materials, and that all research involving human and animal subjects has been approved by the Author's relevant institutional review board.

11. **JoVE Discretion.** If the Author requests the assistance of JoVE in producing the Video in the Author's facility, the Author shall ensure that the presence of JoVE employees, agents or independent contractors is in accordance with the relevant regulations of the Author's institution. If more than one author is listed at the beginning of this Agreement, JoVE may, in its sole

ARTICLE AND VIDEO LICENSE AGREEMENT

discretion, elect not take any action with respect to the Article until such time as it has received complete, executed Article and Video License Agreements from each such author. JoVE reserves the right, in its absolute and sole discretion and without giving any reason therefore, to accept or decline any work submitted to JoVE. JoVE and its employees, agents and independent contractors shall have full, unfettered access to the facilities of the Author or of the Author's institution as necessary to make the Video, whether actually published or not. JoVE has sole discretion as to the method of making and publishing the Materials, including, without limitation, to all decisions regarding editing, lighting, filming, timing of publication, if any, length, quality, content and the like.

12. **Indemnification.** The Author agrees to indemnify JoVE and/or its successors and assigns from and against any and all claims, costs, and expenses, including attorney's fees, arising out of any breach of any warranty or other representations contained herein. The Author further agrees to indemnify and hold harmless JoVE from and against any and all claims, costs, and expenses, including attorney's fees, resulting from the breach by the Author of any representation or warranty contained herein or from allegations or instances of violation of intellectual property rights, damage to the Author's or the Author's institution's facilities, fraud, libel, defamation, research, equipment, experiments, property damage, personal injury, violations of institutional, laboratory, hospital, ethical, human and animal treatment, privacy or other rules, regulations, laws, procedures or guidelines, liabilities and other losses or damages related in any way to the submission of work to JoVE, making of videos by JoVE, or publication in JoVE or elsewhere by JoVE. The Author shall be responsible for, and shall hold JoVE harmless from, damages caused by lack of sterilization, lack of cleanliness or by contamination due to

the making of a video by JoVE its employees, agents or independent contractors. All sterilization, cleanliness or decontamination procedures shall be solely the responsibility of the Author and shall be undertaken at the Author's expense. All indemnifications provided herein shall include JoVE's attorney's fees and costs related to said losses or damages. Such indemnification and holding harmless shall include such losses or damages incurred by, or in connection with, acts or omissions of JoVE, its employees, agents or independent contractors.

13. **Fees.** To cover the cost incurred for publication, JoVE must receive payment before production and publication of the Materials. Payment is due in 21 days of invoice. Should the Materials not be published due to an editorial or production decision, these funds will be returned to the Author. Withdrawal by the Author of any submitted Materials after final peer review approval will result in a US\$1,200 fee to cover pre-production expenses incurred by JoVE. If payment is not received by the completion of filming, production and publication of the Materials will be suspended until payment is received.

14. **Transfer, Governing Law.** This Agreement may be assigned by JoVE and shall inure to the benefits of any of JoVE's successors and assignees. This Agreement shall be governed and construed by the internal laws of the Commonwealth of Massachusetts without giving effect to any conflict of law provision thereunder. This Agreement may be executed in counterparts, each of which shall be deemed an original, but all of which together shall be deemed to be one and the same agreement. A signed copy of this Agreement delivered by facsimile, e-mail or other means of electronic transmission shall be deemed to have the same legal effect as delivery of an original signed copy of this Agreement.